Design and Performance of Sandia's Contactless Coilgun for 50 mm Projectiles*

Ronald J. Kaye, Eugene C. Cnare, M. Cowan,
Billy W. Duggin, Ronald J. Lipinski, and Barry M. Marder
Sandia National Laboratories
Albuquerque, NM 87185-5800

Gary M. Douglas
Rockwell Power Systems, Albuquerque, New Mexico 87102

Kenneth J. Shimp
EG&G, Albuquerque, New Mexico, 87119

Abstract-**A multi-stage, contactless coilgun is being designed to demonstrate the applicability of this technology to accelerate nominal 50 mm (2 inch) diameter projectiles to velocities of 3 km/s. Forty stages of this design (Phase 1 coilgun) will provide a testbed for coil designs and system components while accelerating 200 to 400 gram projectiles to 1 km/s.**

We have successfully qualified the Phase 1 gun by operating 40 stages at half energy (10 kJ stored/stage) accelerating 340 gram, room-temperature, aluminum-armature projectiles to 406 m/s. We expect to accelerate 200 gram projectiles cooled to -196°C to three times this velocity when operating at full energy.

This paper describes the design and performance of the Phase 1 coilgun and includes discussion of coil development, projectile design, capacitor banks, firing system, and integration.

I. INTRODUCTION

Sandia National Laboratories is developing electromagnetic induction launch technology to accelerate payloads to high velocity. The range of interest is 4-6 km/s which is sufficient to cost-effectively launch payloads into low Earth orbit [1]. A 960 m long coilgun type launcher consisting of 9000 coils could accelerate a 1200 kg launch package to deliver a 100 kg payload into low orbit.

Before a goal such as Earth-to-orbit launch can be attempted, the induction launch technology must be shown capable of accelerating projectiles to high velocity. To date, electrically contactless coilguns have achieved only modest velocities on the order of 1 km/s [2-5]. Our goal is to develop a coilgun to accelerate nominal 50 mm diameter, 200 - 400 gram projectiles to 3 km/s. The subject of this paper is our current work of evaluating the designs of the hardware for that coilgun. A 40-stage coilgun (Phase 1) is being tested with a performance goal of accelerating 200 to 400 gram projectiles to 1 km/s.

Our induction coilgun consists of many individually powered solenoidal coils stacked end-to-end over a launch tube which guides a projectile through the coils. A single coil with a section of this tube is shown in Fig. 1 with a 400 gram projectile consisting of an aluminum armature with Teflon[1] boreriders. By sequentially energizing individual coils, a single travelling wave of magnetic energy will pass through the gun at the speed of the accelerated projectile. We call the coilgun contactless because no electrical contact to the armature is necessary. There is, however, intermittent physical contact of the projectile boreriders with the flyway guide tube.

Fig. 2 illustrates schematically how the travelling wave of magnetic field is generated by the coils. The magnitude of the coil currents as well as the induced currents distributed along the length of the solid armature are shown as bar graphs at an instant in time from a calculation by our system model, SLINGSHOT. This code, and its predecessor WARP-10,

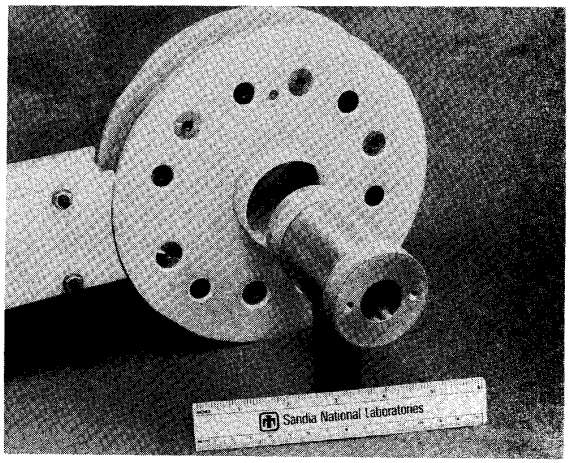

Fig. 1. Single coil assembly with section of flyway tube and projectile.

divides the armature into many single turn circuits and self-consistently solves for the currents in each of these and the coil circuits [6-7]. The capacitor has just switched to the coil marked with an 'X'. The coils to the right are not yet energized and the coil just behind is near peak current. As the projectile passes through the coil just switched, a peak current will be reached to maintain the field applied to the armature. By proper firing of the coils, the travelling wave is slowly varying in the reference frame of the projectile which results in low Ohmic heating of the armature and smooth acceleration.

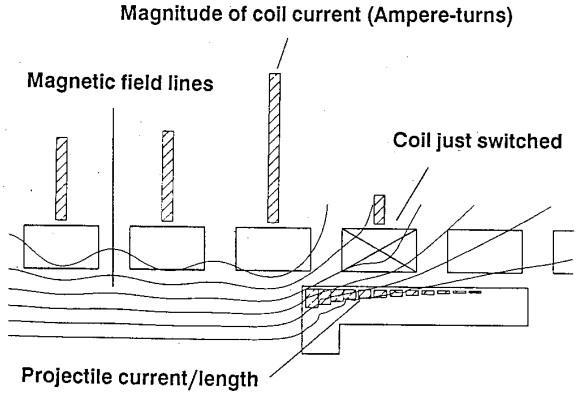

Fig. 2. Coil and projectile currents establish a travelling wave of magnetic field behind the projectile.

*This work was supported by the U.S. Department of Energy under Contract DE-AC04-76DP00789.

[1]Trademark of E.I. Du Pont de Nemours & Co.

The force accelerating the projectile results from the radial component of the magnetic field interacting with the induced azimuthal currents in the armature. However, solution for the magnetic field is not necessary since forces on the projectile can be calculated from the differentials of mutual inductances between armature and coil current elements. Magnetic field lines are shown in Fig. 2 that result from the calculated currents to illustrate the concept only.

To achieve a slowly varying field in the reference frame of the projectile we use SLINGSHOT to account for the diffusion of the current through the armature and determine the appropriate projectile position to energize the coils. An active feedback firing system monitors the projectile position and velocity during the launch and triggers the capacitor discharge into each coil at pre-set projectile positions.

II. COILGUN HARDWARE

A. Major Components of the Assembly

The major components of the 40-stage Phase 1 coilgun are shown in Figs. 3 and 4. Each of the components is only identified here and discussed in later sections.

The coils which form the gun are stacked end-to-end within a steel structure to maintain their alignment and transfer the reaction loads from acceleration to the ground. Each coil is powered by its own switched capacitor located in racks. Coaxial cables connect the individual coils to their respective switches and capacitor. The capacitor, switch, cable, and coil circuit is referred to here as a stage of the coilgun.

At the breech of the gun shown in Fig. 3, pneumatic cylinders we call loaders remove the projectile from a liquid nitrogen bath and push it into the flyway tube of the gun. Although both loaders have been tested, no 40-stage tests have yet utilized cooled projectiles. The loaders are open ended and partially offset from the axis of the flyway tube so that the optical beam of the laser-ranger of the firing system has a clear line of sight to the projectile.

The laser-ranger tracks the location of the projectile during launch in real time and controls the operation of the gun. When the projectile is in the proper position for a given coil to be energized, the firing system sends a trigger to the switch of the appropriate capacitor. Realtime processing of the position data by the firing system also provides velocity diagnostics during launch.

The muzzle velocity is measured using LED-photodiode pairs coupled to the gun through fiber-optic cables. These are shown being installed in Fig. 4.

B. Initial Coil Design

The requirements and criteria for the coils are based on the design goal of accelerating a nominal 50 mm diameter, 400 gram projectile to 3 km/s with an average acceleration of 400 km/s^2. Initial calculations by SLINGSHOT suggests that the overall efficiency in conversion of initial stored energy in the capacitors to projectile kinetic energy could be about 20% at that acceleration with 300 coils spaced apart by approximately half the armature length. The coil parameters based on these estimates for a 300 stage Phase 2 gun are listed in Table I. Parameters with a range of values indicate the variation from the breech to the muzzle of the gun. Parameters are also given for the coils evaluated in the 40-stage Phase 1 coil gun.

Criteria we set for the Phase 2 coil design included:

a) individual coil assemblies supported within a modular structure to allow coil replacement,
b) variable number turns within a fixed length assembly,
c) thin conductors for uniform current distribution,
d) minimal coil radial build to maximize coupling to the armature but sufficient conductor to keep the temperature rise to a maximum of 100°C per pulse,
e) feeds located in a low magnetic field region, and
f) capability to wind multiple parallel wires within the same assembly dimensions with field and current azimuthal symmetry.

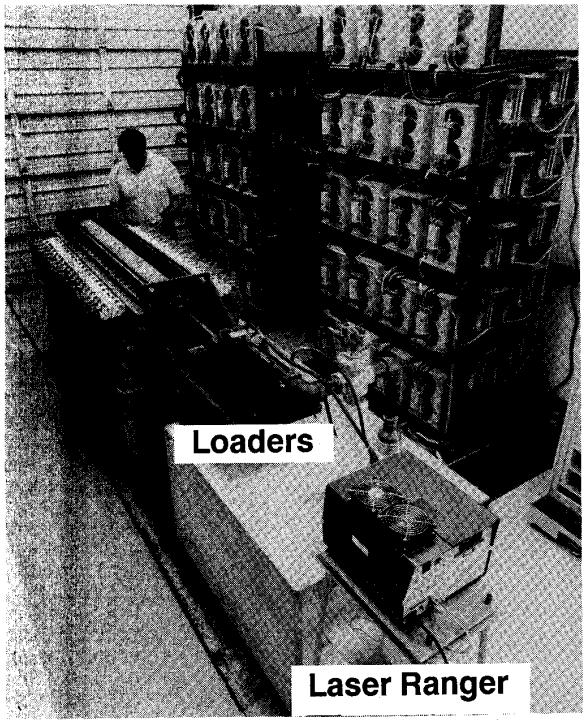

Fig. 3. Breech view of 40-stage Phase 1 coilgun.

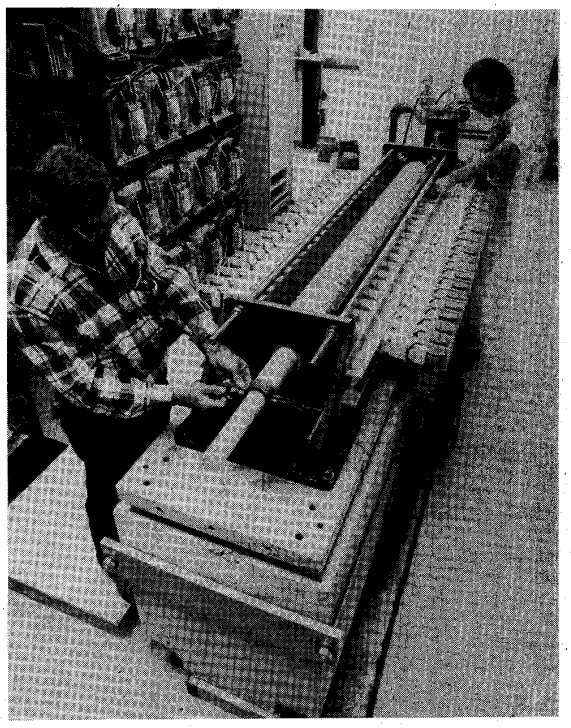

Fig. 4. Muzzle view of 40-stage Phase 1 coilgun.

TABLE I
COIL PARAMETERS AND REQUIREMENTS

	Phase 1	Phase 2
Inner radius	3.1 cm	3.1 cm
Outer radius	4.4 cm	4.4 cm
Length	2.8 cm	2.8 cm
Center to center spacing	4.0 cm	4.0 cm
Number of turns	21	16 - 4
Inductance	30 μH	19 - 1.2 μH
Energy stored/stage	20 kJ	32 kJ
Charge voltage	15 kV	4.5 - 18 kV
Peak current	40 kA	56 - 225 kA
Magnetic field	24 Tesla	28 Tesla
Max radial pressure	85 MPa (12 ksi)	153 MPa (22 ksi)
Max axial pressure	126 MPa (18 ksi)	190 MPa (27 ksi)

For the Phase 1 coilgun we chose to use identical coils and the same capacitance in each stage. The parameters were selected based on available hardware and the expected final velocity of 1 km/s.

The construction of the coil can be seen in the section view of several coil assemblies stacked end-to-end in Fig. 5. Each assembly holds a coil which consists of two spiral windings of 1.27 cm wide, 1.1 mm thick copper ribbon wire. The two windings which contain 10 turns each are connected in series by an additional helical turn at the inner radius of the coil which we call the crossover wire. Feeds are formed by bending the wire in a fold at the outer diameter of the coil for connection to coaxial cables to the capacitor bank. The windings, crossover, and feeds are all constructed from a continuous ribbon wire.

The electromagnetic radial loads on the coil are contained by a thick build of Kevlar[1] 49/epoxy composite wound directly on the windings. These loads cause the copper (UNS C11000, half-hard temper)[2] to yield, but the shape of the winding is maintained by the composite.

Side plates of NEMA[3] grade G-10 laminate are bolted together through the composite to provide electrical insulation and distribute the axial loads between coils. Originally, these plates were to support the flyway tube, but close tolerance requirements of flyway fit could not be met due to plate distortion and movement. The flyway tube is now supported by G-10 spacer disks between coil assemblies.

Axial loads from coil-to-coil coupling and projectile acceleration are transmitted through the side plates of the assembly and neighboring coils to the gun support structure. An axial preload from the structure compresses the coil assemblies while maintaining coil and flyway alignment.

Evaluation of prototypes of the Phase 1 coil design showed promising performance but also indicated potential problems. Tests of coils with static and launched projectiles showed the coils could operate with 20 kJ stored capacitor energy. The winding deformed slightly adjusting to the composite container. Discharging 40 kJ of stored energy into the coil with static projectiles generated over 30 Tesla magnetic fields near the armature, but the winding exhibited more deformation.

Data from these tests and inspection of autopsied coils indicated a higher than expected coil resistance and significant wire edge deformation. Both of these effects were credited to non-uniform current distribution in the winding. The circuit codes, WARP-10 and SLINGSHOT, model the distribution of current in the projectile, but assume uniform current density in the coils. Although the effects of the coil current distribution could be modeled by a circuit code, run-times would preclude practical use of the code for gun simulation.

[2]Unified Numbering System for metals.

[3]National Electric Manufacture's Association

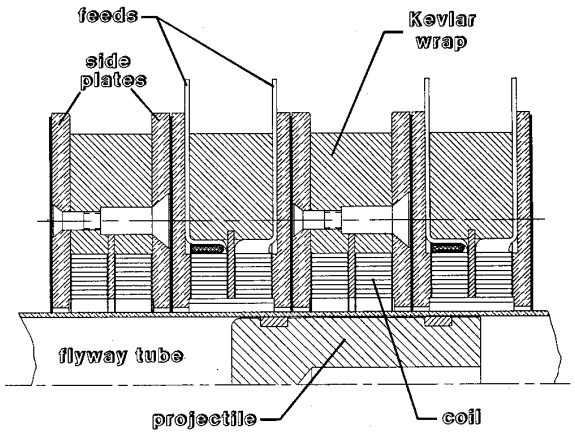

Fig. 5. Section view of 4 coils as stacked in gun with flyway tube and projectile.

To determine the extent of proximity and skin effects on coil current distributions, a time-dependent, magnetic field analysis using the finite-element magnetics code, EMAS[4], was done for the coil geometry in Fig. 5 with a static projectile. A travelling wave was simulated by delaying the current discharge in each of 4 coils in the two-dimensional calculation. The analysis determined that the current density distribution across the width of the wire varied as much as a factor of two, but had little influence on the distribution in the projectile when compared to the solution for a uniform coil current density. The current asymmetry was most pronounced at the mean radius of the coil, not the inner radius. This suggests that the non-uniform current in the coils should not exacerbate the heating in the projectile. The circuit models should be applicable as long as the increased Ohmic losses in the coil are taken into account and the axial force reduction on the projectile due to the coil current distribution is not significant.

Obtaining agreement between SLINGSHOT code calculations and experiments required adjustment to the effective area of coil conductor and coil geometry. However, despite the magnitude of the calculated current density at the wire edges, the heating appeared manageable in autopsied windings.

C. Coil Evaluation in 8-stage Testbed

To further evaluate the coils with combined radial and higher axial loads, an 8-stage coil gun was assembled. This gun was a subset of the hardware and systems to be used in the 40-stage Phase 1 coilgun; except, a simpler support structure held the coils, and a projectile loader was not used. Each of the coils was energized by 171 μF capacitors storing up to 20 kJ and switched by the control of the laser-ranger firing system. Room-temperature, aluminum armature projectiles weighing 384 and 247 grams were accelerated from rest. Eight stages at 20 kJ/stage accelerated the larger mass to 281 m/s and seven stages (6 at 16.7 kJ, 1 at 22 kJ) launched the reduced mass projectile to 314 m/s.

Multiple tests of the coils quickly indicated that the helical crossover wire at the inner radius of the coil was insufficiently supported for the required axial loads. Options to reinforce this part of the winding are limited because of the desire to maintain coupling to the projectile and limit eddy currents in conductive structural elements. After evaluating several concepts for welding the wire of the two windings, copper tabs were successfully welded to the sides of the helical inner turn to provide support for axial loads by the G10 side plates. This essentially made the inner turn the width of both windings for about 14% of the circumference of the crossover turn.

[4]EMAS is Electric and Magnetic Analysis Software licensed from The MacNeal-Schwendler Corp.

The 8-stage tests indicated that the combination of edge heating and axial loads present with a projectile carrying a persistent current and flux will ultimately damage the wire insulation after repeated shots at the desired operating energy. However, the winding damage is significantly less at lower operating energy. Considering the need to evaluate the other major components of the gun (capacitor bank, firing system, and coil support structure) and verify the circuit model, we decided to use this coil for the Phase 1 gun. For evaluating launcher components, the gun operates at 10 kJ/stage, but will operate at 20 kJ/stage for a limited number of performance tests. Meanwhile, a new coil is being developed on a parallel path.

D. Litz Wire Coil Design

A new coil design for the Phase 1 gun which uses litz wire looks promising as a replacement to the initial design wound with ribbon wire. Litz wire provides a uniform coil current density which will eliminate localized edge heating of the wire, reduce the deformation of the winding at the edges, and allow the coil to be accurately modeled by SLINGSHOT. A coil constructed by axially winding litz wire will eliminate the crossover wire problem. The geometry of the winding is very similar to what we used in our 144 mm, 6-stage coilgun [8]. The critical issue is whether the mechanically weak litz wire, which has desirable electrical properties, can be made sufficiently strong to withstand the stresses during launch.

Litz wire has been used for coils and projectiles in several guns at 25 Tesla or more [4, 9-10]. Thanks to the generous cooperation of Jim Andrews and Don Bresie at the Univ. of Texas at Austin, Center for Electromechanics, we were able to quickly develop our techniques for winding and vacuum encapsulating rectangular-compacted litz wire coils which are tightly wound edgewise. Tests of our first coils of this construction showed that litz wire, when properly encapsulated, will form a robust structure which we expect to be capable of handling the loads anticipated in Table I.

Currently we are evaluating potting compounds for coil strength and shot life. Mechanical stress analysis and instrumented testing of prototype coils are in progress to develop the mechanical model for litz wire/epoxy composite. Single stage coil tests with static projectiles have generated 28 Tesla fields at the coil inner radius without significant deformation of the winding. Multi-stage tests with static projectiles are planned to simulate the peak loads during a launch prior to replacing the ribbon wire coils in the Phase 1 coilgun.

E. Projectile and Flyway Tube

The projectile launched in the Phase 1 coilgun is an 7075-T73 aluminum armature with Teflon boreriders. The 86 mm long cylinder is partially hollowed out to reduce mass with the tube section at the leading edge. The rear is solid to provide a surface on axis for the reflector required by the laser-ranger and minimize deformation of the projectile during launch.

The flyway tube shown in Fig. 1 is a 1.5 mm thick, convolute-wound fiberglass/epoxy tube whose outer diameter has been machined. The gun uses a nominal 2.3 m long flyway which can be removed without dismantling the gun. Both single and jointed tubes have been successfully tested up to projectile velocities of a few hundred meters/second.

The initial tests of the gun were conducted with 51.0 mm inner diameter (ID) tubes, 50.4 mm outer diameter (OD) projectile boreriders, and 49.9 mm OD armature weighing 384 grams. However, slight deformation and movement of the side plates of the coil assemblies deformed the tube causing excessive borerider and tube wear. To decouple the tube from the side plates, we installed spacer disks between the coils to support the tube. However, this required the bore diameter to be reduced. We now use 47.6 mm ID tubes, and launch projectiles with 47.2 mm OD boreriders and 46.7 mm OD armature weighing 347 grams.

F. Capacitor Banks

Each of the coils of the 40-stage Phase 1 coilgun is powered by its own capacitor bank. A 40 kJ, 176 μF capacitor is switched by a National Electronics 7703 EHV ignitron through 3 parallel Belden YK-198 coaxial cables to the coil. The first 20 stages of the launcher have another 7703 EHV ignitron to crowbar the coil at peak current. Each circuit is grounded at the cathode of the main ignitron which is common to the cathode of the crowbar ignitron.

At 20 kJ of energy stored per stage, each capacitor stores about 2.6 Coulombs. The main ignitron of a non-crowbarred circuit or the crowbar ignitron of a crowbarred circuit transfer about 10 times the stored charge and carry a peak current of 35 - 40 kA. Although these operating parameters strain the capabilities of these ignitrons, their reduced lifetime should be sufficient for the expected life of Phase 1 testing.

Each capacitor is connected through a combination charge/dump copper-sulfate solution resistor to a common buss that can be grounded to dump the banks or attached to a high-voltage power supply to charge the banks. These resistors isolate the banks during charging in the event a switch pre-fires and during the sequential firing of the coil stages during a launch. The RC time constant of each circuit is about 0.34 seconds which allows the banks to quickly equilibrate during a charging pre-fire, yet is sufficiently long compared to the few milliseconds time between firing of the first and last stages during projectile launch.

G. Firing System

The laser-ranger shown in Fig. 3 is a real-time, phase-shift analyzer capable of detecting a target position with a resolution of 2.4 mm over a range of about 50 m. The projectile position in the gun flyway tube is obtained by reflecting a modulated laser beam off a reflective material that has been attached to the projectile's surface. Position versus time information is then transmitted to the control room over a fiber optic link where the remaining firing system control logic is located.

Control logic circuits compare the projectile position data to firing positions assigned to each coil stage. Firing positions are determined before the shot from calculations by SLINGSHOT and preset into the system. When the projectile reaches the firing position for a coil stage, the logic circuits deliver a 50 V pulse to trigger the capacitor bank switch and any appropriate instrumentation. At the present time the firing system can separately trigger 50 individual coil stages at projectile velocities up to 560 m/s. Additions and modifications to the system will allow 300 stages to be triggered with projectile velocities up to 4 km/s.

The control logic of the firing system also has the option of setting a velocity window for each firing pulse circuit. The logic computes the average velocity of the projectile between each pre-set firing position, and if this velocity is out of the range of the user set window for that interval, a firing pulse will not be produced for that coil stage. Since the control logic circuits operate in groups of ten, the fire pulse is also inhibited in any of the following stages in that group.

The vertical loading tray is depicted in Fig. 6 removing the projectile from a liquid nitrogen bath. Prior to a shot, the projectile can be submersed in a bath of liquid nitrogen (LN2) and temperature stabilized to reduce armature resistivity. At the time of shot firing, the projectile is raised into the loader tube and the firing system establishes the projectile position. If the reflected power is above a minimum level to produce reliable operation, the ranger will indicate it is ready for operation. Dry nitrogen is passed over the reflector surface after removal from the LN2 bath to reduce the frost build up on the reflector material.

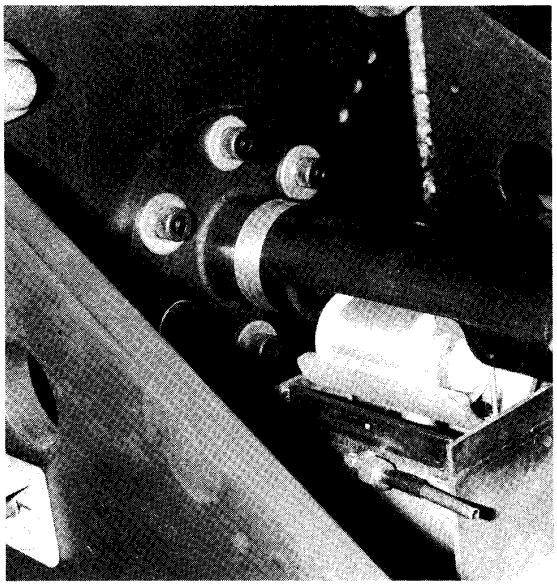

Fig. 6. Projectile elevated from liquid nitrogen bath into loader tube.

III. Phase 1 Coilgun Performance

Following assembly of the gun in early November 1991, we began diagnostic tests to evaluate system components beginning with 10 stages and are now operating 40 stages. To maximize coil lifetime, these tests are done at 10 kJ stored/stage which is half the desired operating energy. Following these system evaluation tests, the energy on all stages will be increased to 20 kJ/stage.

The diagnostic tests uncovered problems with some parts of the gun and proved the performance of others. Insufficient stiffness in the steel support structure aligning the coils and flyway resulted in greater projectile-borerider and flyway tube wear than expected at 300 m/s. Modifications to the structure and method of flyway tube support eliminated this problem.

The capability of the firing system to shut down the gun if the projectile velocity is out of an allowed range during a launch has been proven. This shutdown feature is illustrated in Fig. 7 where projectile velocity is plotted versus its position in the gun. The data is the first time-derivative of the laser-ranger measured projectile position plotted with a SLINGSHOT code simulation of the test. In this test, projectile velocity exceeded the allowed range of velocity at stage 21 causing the next 10 stages to shut down. A wider allowed range at stage 31 resumed firing of the last 10 stages. The allowed range of velocity set for a shot depends upon the nature of the test and estimated risk to hardware should the gun not perform as expected. We have operated with ranges from 10% to 30% around the code predicted values.

The SLINGSHOT code-predicted velocity plotted in Fig. 7 agrees fairly well with the data from a test that has varying conditions. The 10 m/s peak-to-peak oscillation in the data is an artifact of the laser-ranger. Coils in stages 1-15 were crowbarred at peak current on this test while the currents were allowed to ring in all other stages. The code also properly accounts for the shutdown of stages 21-30. Code agreement with data is generally within 10% or better. The fact that the coil current density is not uniform, especially with non-crowbarred currents is believed to cause this discrepancy.

Projectile velocity data from a test of all 40 stages is shown in Fig. 8 compared to the SLINGSHOT calculations. In this test, stage 3 did not fire and the calculation performed after the shot includes that effect. The pre-shot calculation for all 40 stages has only a slightly higher velocity.

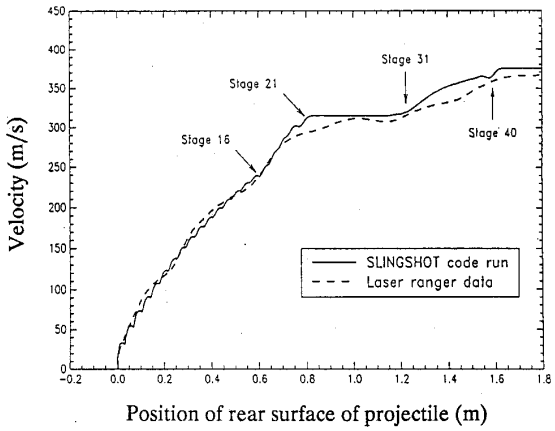

Fig. 7. Projectile velocity versus position code estimate and data for test of stages 1-20 and 31-40 operating at 10 kJ stored per stage.

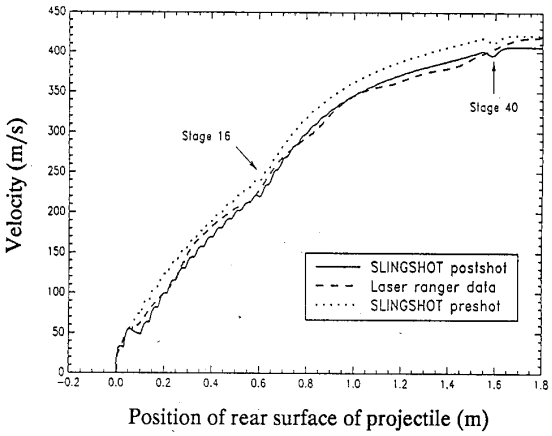

Fig. 8. Projectile velocity versus position code estimates and data for test of 39 of 40 stages operating at 10 kJ stored per stage.

Since the Phase 1 gun is designed for operating at a single frequency launching 400 gram projectiles at 20 kJ stored per stage, operating at lower energy results in lower velocity and efficiency. The data shown in Figs. 7 and 8 are from operation at 10 kJ/stage accelerating a 339 gram, 46.7 mm OD, room-temperature projectiles which yields a stored-to-kinetic conversion efficiencies of 7%. Operating 40 stages at 20 kJ/stage, we expect a 200 gram projectile of the same OD cooled to -196°C to be accelerated to about 1.1 km/s with a 15% conversion efficiency.

IV. Summary

A multi-stage, contactless coilgun is being designed to demonstrate the applicability of this technology to accelerate nominal 50 mm (2 inch) diameter projectiles to velocities of 3 km/s. Forty stages of this design are assembled as our Phase 1 coilgun to provide a testbed for coil designs and system components.

We have successfully qualified the Phase 1 gun by operating 40 stages at half energy (10 kJ stored/stage) accelerating 340 gram, room-temperature, aluminum-armature projectiles to 406 m/s. We expect to accelerate 200 gram projectiles cooled to -196°C to three times this velocity when operating at full energy.

ACKNOWLEDGMENT

The authors thank the team of Robert Davis, Roque Feliciano, Edward Ratliff, and Robin Sharpe for their contributions to design and fabrication of hardware and operation of the gun. Thanks also to the significant effort in coil fabrication by Mabel Pecos, Meliton Gonzales, Ernie Corea, Fred Hooper, and Henry Martinez. Support from Dean Rovang (EMAS calculations and composite analysis), Howard Arris and Ken Wischmann (litz coils), Isaac Shokair (SLINGSHOT calculations and analysis), and Keith Tolk (review) is greatly appreciated.

REFERENCES

[1] R. J. Lipinski, et al., "Space applications for contactless coilguns," presented at the 6th Symposium on Electromagnetic Launch Technology, Austin, Texas, April 28-30, 1992, [unpublished].

[2] M. Cowan et al., "Exploratory development of the reconnection launcher, 1986-1989," *IEEE Trans. on Magnetics*, vol. 27, no. 1, pp. 563-567, January 1991.

[3] Z. Zabar et al., "Test results for three prototype models of a linear induction launcher," *IEEE Trans. on Magnetics*, vol. 27, no. 1, pp. 558-562, January 1991.

[4] M. W. Ingram, J. A. Andrews, D. A. Bresie, "An actively switched pulsed induction accelerator," *IEEE Trans. on Magnetics*, vol. 27, no. 1, pp. 591-595, January 1991.

[5] K. McKinney and P. Mongeau, "Multiple stage pulsed induction acceleration," *IEEE Trans. on Magnetics*, vol. 20, no. 2, pp. 239-242, March 1984.

[6] B. M. Marder, "A coilgun design primer," presented at the 6th Symposium on Electromagnetic Launch Technology, Austin, Texas, April 28-30, 1992, [unpublished].

[7] M. M. Widner, "Warp-10: a numerical simulation model for the cylindrical reconnection launcher," *IEEE Trans. on Magnetics*, vol. 27, no. 1, pp. 634-638, January 1991.

[8] R. J. Kaye et al., "Design and performance of a multi-stage reconnection launcher," *IEEE Trans. on Magnetics*, vol. 27, no. 1, pp. 596-600, January 1991.

[9] P. P. Mongeau, "Inductively commutated coilguns," *IEEE Trans. on Magnetics*, vol. 27, no. 1, pp. 568-572, January 1991.

[10] J. A. Andrews and J. R. Devine, "Armature design for coaxial induction launchers," *IEEE Trans. on Magnetics*, vol. 27, no. 1, pp. 639-643, January 1991.